

1 **Deglaciation of the Caucasus Mountains, Russia / Georgia, in the 21st century observed**
2 **with ASTER satellite imagery and aerial photography**

3

4 Maria Shahgedanova¹, Gennady Nosenko², Stanislav Kutuzov^{1,2}, Oksana Rototaeva² and Tatyana
5 Khromova²

6 ¹Department of Geography and Environmental Science and Walker Institute for Climate System
7 Research, University of Reading, Whiteknights, Reading RG6 6AB, UK.

8 ²Laboratory of Glaciology, Institute of Geography, Russian Academy of Sciences, 29
9 Staromonetny Pereulok, Moscow, 119017, Russia. Tel: +7 499 1259011; Fax: +7 495 9590033;

10 Correspondence to: M. Shahgedanova (m.shahgedanova@reading.ac.uk)

11

12 **Abstract**

13 Changes in map area of 498 glaciers located on the Main Caucasus Ridge (MCR) and on Mt.
14 Elbrus in the Greater Caucasus Mountains (Russia and Georgia) were assessed using
15 multispectral ASTER and panchromatic Landsat imagery with 15 m spatial resolution from
16 1999-2001 and 2010-2012. Changes in recession rates of glacier snouts between 1987-2001 and
17 2001-2010 were investigated using aerial photography and ASTER imagery for a sub-sample of
18 44 glaciers. In total, glacier area declined by $4.7 \pm 2.1\%$ or $19.2 \pm 8.7 \text{ km}^2$ from $407.3 \pm 5.4 \text{ km}^2$ to
19 $388.1 \pm 5.2 \text{ km}^2$. Glaciers located in the central and western MCR lost $13.4 \pm 7.3 \text{ km}^2$ ($4.7 \pm 2.5\%$)
20 in total or 8.5 km^2 ($5.0 \pm 2.4\%$) and 4.9 km^2 ($4.1 \pm 2.7\%$) respectively. Glaciers on Mt. Elbrus,
21 although located at higher elevations, lost $5.8 \pm 1.4 \text{ km}^2$ ($4.9 \pm 1.2\%$) of their total area. The
22 recession rates of valley glacier terminus increased between 1987 - 2000/01 and 2000/01 - 2010
23 from $3.8 \pm 0.8 \text{ m a}^{-1}$, $3.2 \pm 0.9 \text{ m a}^{-1}$ and $8.3 \pm 0.8 \text{ m a}^{-1}$ to $11.9 \pm 1.1 \text{ m a}^{-1}$, $8.7 \pm 1.1 \text{ m a}^{-1}$ and

24 14.1±1.1 m a⁻¹ in the central and western MCR and on Mt. Elbrus respectively. The highest rate
25 of increase in glacier termini retreat was registered on the southern slope of the central MCR
26 where it has tripled. A positive trend in summer temperatures forced glacier recession and strong
27 positive temperature anomalies of 1998, 2006, and 2010 contributed to the enhanced loss of ice.
28 An increase in accumulation season precipitation observed in the northern MCR since the mid-
29 1980s has not compensated for the effects of summer warming while the negative precipitation
30 anomalies, observed on the south slope of the central MCR in the 1990s, resulted in stronger
31 glacier wastage.

32

33 **1 Introduction**

34 Shrinkage of mountain glaciers in response to the observed climatic warming has been
35 documented worldwide. The 1990s and 2000s were the warmest decades in the 150-year
36 instrumental record (IPCC, 2013; see their Fig. 2.19), with global surface temperature anomalies
37 of 0.24°C and 0.44°C above the 1961-1990 mean respectively
38 (www.metoffice.gov.uk/research/monitoring/climate/surface-temperature). Mountain glaciers are
39 sensitive indicators of climatic change at the decadal time scale (Hoelzle et al., 2003) and
40 acceleration in their area and volume reduction in the 1990s has been reported for many regions
41 (Dyurgerov and Meier, 2000; Zemp et al., 2009). The contribution of glaciers and ice caps
42 (excluding Antarctica and Greenland) to the global sea level budget increased from 0.67±0.03
43 mm a⁻¹ in 1972-2008 to 0.99±0.04 mm a⁻¹ in 1998-2008, in line with intensifying climatic
44 warming and glacier melt (Church et al., 2012).

45 Remote sensing is an established way of monitoring changes in glacier area and positions of
46 glacier snouts. To date, most assessments have been conducted using multispectral Landsat

47 Thematic Mapper (TM) and Enhanced Thematic Mapper Plus (ETM+) imagery, with 30 m
48 horizontal resolution available since 1982 and 1999 respectively, and Advanced Spaceborne
49 Thermal Emission and Reflection Radiometer (ASTER) imagery with 15 m resolution available
50 since 2000. Together with historical aerial photographs and maps, this imagery enabled
51 assessments at time steps of 20-50 years during which magnitude of glacier change significantly
52 exceeded measurement errors. Various studies that used Landsat imagery reported measurement
53 errors from about 3-5% of single-glacier area change for clear ice (with larger errors for smaller
54 glaciers) to over 10% for debris-covered glaciers or those whose outlines merge with snow fields
55 (e.g. Andreassen et al., 2008; Paul and Andreassen, 2009; Bhambri et al., 2011; Paul et al.,
56 2013). For this reason, assessments at shorter intervals in most regions required data from
57 repeated aerial surveys or finer-resolution satellite imagery whose spatial extent and availability
58 are limited (e.g. Hall et al., 2003). Now, when high-resolution multispectral ASTER imagery has
59 been available for more than a decade, its consistent use should significantly reduce uncertainties
60 in measurements of glacier change and enable assessments at decadal intervals over wider
61 regions.

62 One of the main centres of mountain glaciation in Europe is the Greater Caucasus Mountains
63 located between the Black and Caspian Seas in the densely populated south-western Russia and
64 Georgia (Fig. 1). Few studies of the Caucasus glaciers have examined large samples using
65 consistent methods and data. In the Russian-language literature, the most detailed assessments
66 are those by Panov (1993) and Yefremov et al. (2007) based predominantly on repeated field
67 measurements of positions of glacier termini in the Main (Glavny) Caucasus Ridge (MCR). In
68 the English-language literature, Stokes et al. (2006) examined changes in termini positions of
69 113 glaciers in the central Greater Caucasus between 1985 and 2000 using satellite imagery.

70 Panov's (1993) analysis of the field measurements and data derived from analysis of historical
71 maps showed that in the period between 1933 and 1965/70 glacier termini in the MCR retreated
72 at an average rate of 12.3 m a^{-1} while in the period between 1965/70 and 1986/89 the recession
73 slowed down to 6.1 m a^{-1} . In the former assessment period, glaciers of the northern and southern
74 slopes retreated at the same rate while in the latter period, the retreat rate of 8.9 m a^{-1} observed
75 on the southern slope exceeded the retreat rate of 4.8 m a^{-1} observed on the northern slope.
76 Stokes et al. (2006) reported average glacier termini recession rates of 8 m a^{-1} between 1985 and
77 2000. From this assessment, they inferred a total loss of bare ice area of about 10% but the study
78 did not assess changes in areas of individual glaciers. Yefremov et al. (2007) reported similar
79 results based on field measurements. Both Stokes et al. (2006) and Yefremov et al. (2007)
80 reported acceleration of glacier retreat in the 1990s although Yefremov et al. (2007) stressed
81 equally high recession rates in the mid-20th Century and slow down in glacier retreat between
82 1965 and 1985 in line with the earlier work by Panov (1993).

83 Other studies focused on changes in area and fluctuation of termini of individual or small
84 samples of glaciers. Popovnin and Petrakov (2005) provided a detailed history of shrinkage of
85 Djankuat Glacier in the central sector of the MCR between 1968 and 1999 reporting 9% (0.29%
86 a^{-1}) shrinkage. Kutuzov et al. (2012) examined changes in Marukh Glacier located in the western
87 MCR showing that area reduction was similar at 17% between 1945 and 2011 ($0.25\% \text{ a}^{-1}$).
88 Bushueva and Solomina (2012) examined recession of Kaskatash Glacier in the central MCR
89 showing acceleration of its snout retreat rate from 1.8 m a^{-1} between 1971 and 1987 to 7.5 m a^{-1}
90 between 1987 and 2008. More recently, changes in lengths of seven glaciers in the central
91 greater Caucasus over the last 200 years were analysed showing that over the period these

92 glaciers retreated with the exception of 1910-1920s and 1960-1980s, and that the rate of retreat
93 increased since the 1990s (Lerclerq et al., 2014).

94 Changes in glacierized area on Mt. Elbrus, the largest glacierized massif in the Caucasus (Fig.
95 1), were examined by Zolotarev and Kharkovets (2007) who reported glacier shrinkage between
96 1957 and 1997. More recently, Zolotarev and Kharkovets (2012) extended these assessments to
97 2007 using data from field measurements, aerial photography and high-resolution Cartosat-1
98 imagery. According to their assessments, the total glacierized area on Mt. Elbrus declined from
99 132.51 km^2 in 1957 to 120.03 km^2 in 2007. Glacierized area declined by $0.22 \text{ km}^2 \text{ a}^{-1}$ between
100 1957 and 1979, by $0.16 \text{ km}^2 \text{ a}^{-1}$ between 1979 and 1997, and by $0.45 \text{ km}^2 \text{ a}^{-1}$ between 1997 and
101 2007. Another assessment of glacier change on Mt. Elbrus was published by Holobaca (2013)
102 reporting area change of 9.1% between 1985 and 2007 from Landsat TM imager.

103 Continuous observations of glacier mass balance are conducted at two reference glaciers,
104 Djankuat and Garabashi (WGMS, 2013). Strong reductions in cumulative mass balance were
105 registered at both since 1995 providing further evidence of glacier wastage (Popovnin, 2000;
106 Popovnin and Petrakov, 2005; Shahgedanova et al., 2005; 2007; Rototaeva et al., 2006; Dolgova
107 et al., 2013).

108 While published assessments suggest that glaciers in the Greater Caucasus are retreating and
109 rates of retreat have accelerated at the end of the 20th century, reliable large-scale assessments of
110 changes in map areas of glaciers are not available with the exception of those by Zolotarev and
111 Kharkovets (2007; 2012) for Mt. Elbrus.

112 This paper has two objectives: (i) to quantify changes in glacier map area in the central and
113 western sectors of the Greater Caucasus Mountains between 1999/2001 and 2010/2012 using
114 ASTER imagery (or, where not available, 15-m resolution panchromatic Landsat imagery) in

115 line with the requirements of the Global Land Ice Measurements from Space (GLIMS) project
116 (<http://www.glims.org/>) and (ii) to assess changes in glacier retreat rates from the end of the 20th
117 Century to the end of the first decade of the 21st century using aerial photographs from 1987 and
118 ASTER imagery for a sub-sample of valley glaciers. Glacier snout recession is a more sensitive
119 indicator of changes at decadal time scale than area change (Hoelzle et al., 2003; Koblet et al.,
120 2010; Bhambri et al., 2012; Leclerq and Oerlemans, 2012; Leclerq et al., 2014) especially for the
121 large glacierized massifs such as Mt. Elbrus. Valley glaciers were selected for the assessment
122 because they exhibit the clearest climatic signal, being less dependent on avalanche nourishment
123 and topography than other types of glaciers (e.g. Shahgedanova et al., 2012).

124

125 **2 Study region**

126 According to the Catalogue of Glaciers of the USSR (Panov and Kravtsova, 1967; Borovik and
127 Kravtsova, 1970; Maruashvili et al., 1975) and the World Glacier Inventory (WGI), the Greater
128 Caucasus accommodated over 2000 glaciers with a combined area of approximately 1600 km² in
129 the 1960s-1980s (http://nsidc.org/data/glacier_inventory/). Very close results were obtained by
130 Nakano et al. (2013) from Landsat imagery. GLIMS (www.glims.org) and Randolph Glacier
131 Inventory (Arendt et al., 2012) quote over 1300 glaciers with a combined area of 1354 km². The
132 difference is due to the omission of the smaller glaciers in the eastern sector of the Caucasus in
133 this recent assessment.

134 The Greater Caucasus is subdivided into western, central and eastern sectors which have
135 average elevations of 3200 m, 4100 m, and 3700 m respectively. The most elevated central
136 sector extends between Mt. Elbrus (5642 m a.s.l.; Fig. 1) located several km north of the MCR
137 and Mt. Kazbek (5033 m a.s.l.; 42.7°N; 44.52°E). A characteristic feature of the Greater

138 Caucasus is a strong west-east precipitation gradient. The southern slope of the western MCR
139 receives over 2000 mm of precipitation while in the east, the annual total is about ten times lower
140 (Volodicheva, 2002). In response to the west-east precipitation gradients, the equilibrium line
141 altitude (ELA) changes rising from 2500-2700 m in the west through about 3200-3400 m in the
142 central sector to 3700-3950 m in the east. Due to greater precipitation in the south, ELA is lower
143 on the southern slopes especially in the central MCR and on Mt. Elbrus, where differences
144 between the southern and northern slopes reach 1000 m and 200-300 m respectively (Rototaeva
145 et al., 2006).

146 The largest glaciers are located in the central Greater Caucasus including the glaciated massif
147 of Mt. Elbrus. A number of larger valley glaciers have individual areas of 3-36 km². Cirque
148 glaciers with individual areas of 1 km² or less account for approximately 40% of the total. In the
149 western and eastern sectors, cirque glaciers with individual areas less than 3 km² prevail
150 (Rototaeva et al., 2006).

151

152 **3 Data and methods**

153 Changes in glacierized area and recession rates of glacier termini were assessed for the central
154 and western sectors of the MCR and Mt. Elbrus (Table 1; Fig. 1). Areas of 498 glaciers were
155 mapped of which 174 and 304 were located in the central and western sectors of the MCR
156 respectively on both northern (Russia) and southern (Georgia) slopes and twenty on Mt. Elbrus
157 (Table 1). The size of the smallest glacier mapped was 0.02 km².

158 Glacier outlines were mapped manually despite the advantages of automated mapping
159 demonstrated by Paul et al. (2009; 2013) because of the failure of the SWIR channel used in
160 automated classifications (Paul et al., 2002; Bolch et al., 2010) on ASTER in April 2008.

161 Potential relative error strongly increases with decreasing glacier area and manual corrections are
162 required when automatically mapping small glaciers because automated techniques tend to omit
163 mixed (clear ice – debris cover) pixels along the glacier perimeter resulting in a systematic
164 negative bias in glacier area calculation. Paul et al. (2013) and Fischer et al. (2014) have shown
165 that the bias significantly increases for glaciers with areas less than 1 km² (which constitute
166 about 85% of all glaciers in the Caucasus) reducing the advantages of automated techniques.

167

168 **3.1 Satellite imagery and glacier area mapping**

169 Two ASTER scenes from 2001 and 2010 were used for glacier mapping in the central MCR
170 (Table 1). ASTER imagery from 2010 was used for mapping glaciers in the western MCR,
171 however, earlier cloud-free imagery was not available and a Landsat ETM+ panchromatic image
172 from 2000, which has the same resolution of 15 m as ASTER, was used instead. For Mt. Elbrus,
173 ASTER scene was used for 2012 and panchromatic Landsat ETM+ was used for 1999 because
174 these are the only higher-resolution cloud-free images which cover the whole of Mt. Elbrus. An
175 ASTER 2001 scene, used for mapping in the central MCR, covers only the south-eastern sector
176 of Mt. Elbrus. To aid glacier mapping, a vast database of ground-based and aerial oblique
177 photographs was used (e.g. Fig. 2, 3).

178 The ASTER images were supplied by NASA Land Processes Distributed Active Archive
179 Center (LP DAAC) and Landsat ETM+ panchromatic images were downloaded from the US
180 Geological Survey (USGS; <http://glovis.usgs.gov/>). Both were supplied in the Universal
181 Transverse Mercator (UTM) zones 36-38 WGS 84 projection. The ASTER images were
182 orthorectified prior to the distribution (Lang and Welch, 1999). All satellite images were
183 acquired under [nearly] cloud-free conditions at the end of the ablation season (Table 1) when

184 glacier tongues were free of seasonal snow. On ASTER images, glacier outlines were mapped
185 using the 0.52-0.6 μm , 0.63-0.69 μm , and 0.78-0.86 μm bands. Where glacier margins were
186 obscured by shadows from rocks and glacier cirque walls, a contrast-stretching function was
187 applied to the imagery using ENVI 4.6 software.

188 Most glaciers, except those located on Mt. Elbrus, have clearly defined ice divides. To avoid
189 errors associated with delineation of the upper boundaries of glaciers located on Mt. Elbrus, the
190 total glacierized area of the Elbrus massif was mapped and reported as the main outcome of this
191 study. To assess changes in individual glaciers, the ASTER GDEM and the hydrological tools
192 for basin delineation available in ARC 10.1 GIS and applied previously by Schiefer et al. (2008),
193 Paul and Andreassen (2009), Svoboda and Paul (2009), Bolch et al. (2010) and Keinholz et al.
194 (2013) and were used for glacier delineation. It was assumed that upper boundaries of glaciers on
195 Mt. Elbrus did not change between 1999 and 2012.

196 Within the study area five glaciers have been identified as surging by Rototaeva (2006). These
197 glaciers were excluded from the analysis with the exception of the Kyukyurtlyu glacier located
198 on Mt. Elbrus. Although this glacier can exhibit changes that are not forced by climatic
199 variations, there was no evidence of surging within the assessment period. Of the remaining four,
200 three glaciers did not exhibit measurable change within the assessment period and one (Cheget-
201 Kara) lost 0.04 km^2 or 1.5% of its area despite advancing by approximately 40 m between 2000
202 and 2003 (Rototaeva, 2006).

203

204 **3.2 Quantification of errors**

205 For each glacier located in the MCR, we calculated three error terms resulting from (i) co-
206 registration of images, (ii) identification of glacier margins, and (iii) presence of debris cover on
207 glacier snouts.

208 The ASTER images, used for mapping glaciers in the central sector of the MCR, and ASTER
209 and panchromatic Landsat ETM+ images, used for mapping in the western sector of the MCR
210 and Mt. Elbrus, were co-registered using a network of 12 ground control points (GCP) for each
211 pair of images. Although ASTER imagery was used for both 2001 and 2010, co-registration of
212 these images and calculation of the resulting error term were required because different DEMs
213 were used in 2001 and 2010 (Meyer et al., 2011). The maximum root-mean-square error
214 ($RMSE_{x,y}$) was 8.1 m, which is less than the size of an ASTER pixel. The error of co-registration
215 was calculated following Granshaw and Fountain (2006). A buffer, with a width of half of the
216 $RMSE_{x,y}$ was created along the glacier outlines and the error term was calculated as an average
217 ratio of the original glacier areas to the areas with a buffer increment, resulting in an average
218 error of $\pm 1.2\%$. The errors of co-registration of ASTER and panchromatic Landsat ETM+
219 images used for mapping glaciers in the western MCR and on Mt. Elbrus were calculated using a
220 similar method. In the western Caucasus, $RMSE_{x,y}$ of 8.3 m and the error of $\pm 1.4\%$ were
221 achieved while on Mt. Elbrus, where the glacierized area is an order of magnitude larger than the
222 size of individual glaciers in the MCR, the error was $\pm 0.7\%$.

223 The uncertainty of glacier margin identification was estimated using multiple digitization
224 following Paul et al. (2013). A sub-sample of twenty glaciers from the MCR with areas of 0.5 -
225 9.8 km² was re-digitised ten times by three different operators. The average error was calculated
226 as 1.3% and used for the central and western MCR sub-samples. The error for the Elbrus
227 glacierized massif as a whole was very small at 0.2% due to (i) its large size and (ii) detailed

228 knowledge of the region obtained during many seasons of field work, including DGPS surveys
229 conducted since 2008 on individual glaciers (unpublished field records) and recent helicopter
230 surveys (e.g. Fig. 2).

231 Debris cover on glacier snouts is a major source of error in glacier mapping (Bhambri et al.,
232 2011; Bolch et al., 2008; Racoviteanu et al., 2008; Frey et al. 2012; Paul et al., 2013). In the
233 Caucasus, supra-glacial debris cover has lesser extent than in many glacierized regions,
234 especially in Asia (Stokes et al., 2007). Importantly, debris cover is not continuous on the snouts
235 of many glaciers in the MCR and most glaciers of Mt. Elbrus (Fig. 2). Most debris-covered
236 snouts do not merge with periglacial landforms, exhibiting a marked change in topography, and
237 are characterised by the presence of patches of clear ice and/or thermoscarst making
238 identification of glacier margins on the satellite imagery easier.

239 To account for the error term due to debris cover, we followed Frey et al. (2012) and
240 increased the buffer size to two pixels (30 m) for the debris-covered segments of those glaciers
241 where supra-glacial debris was extensive. One of the most heavily debris-covered glaciers in the
242 Caucasus is Donguz-Orun (glacier tongue coordinates 43.231°N; 42.512°E) where supra-glacial
243 debris cover approximately 70% of the glacier as a result of avalanche nourishment supplying
244 debris from the headwall exceeding 4400 m a.s.l. (Fig. 3). For this specific glacier, the error of
245 mapping due to debris cover was calculated as $\pm 4.7\%$. We stress that (i) this glacier is not typical
246 of the region and (ii) this is the largest error in the whole data set. The debris cover term was
247 calculated for 67 glaciers and for most glaciers, it was below $\pm 1\%$.

248 The total error of glacier area change was calculated as a root mean square of the co-
249 registration, margin identification and, where applicable, debris-cover-related error terms.

250

251 **3.3 Assessment of changes in positions of glacier termini using aerial photographs**

252 Positions of the termini of 21 and 17 valley glaciers located in the central and western sectors of
253 the MCR respectively and of 6 glaciers located on the south-eastern slope of Mt. Elbrus were
254 measured on the satellite images and on the aerial photographs from 1987 (Table 1). The number
255 of measured valley glaciers (44 out of 97 in the sample) was restricted by the availability of
256 suitable aerial photographs. Glacier length and slope are the main controls of glacier snout
257 reaction (Hoelzle et al., 2003). All glaciers in the sample had similar slopes; the average lengths
258 (measured along the central flow line) of glaciers and length ranges are shown in Table 5.

259 Twenty six and seventeen aerial photographs with a resolution of 1-3 m were obtained on 25-
260 26 September 1987 under the nearly cloud-free conditions for central (including Mt. Elbrus) and
261 western sectors of the Greater Caucasus respectively (Table 1). The photographs were digitized
262 at 600 dpi resolution and co-registered to the 2001 ASTER and the 2000 Landsat ETM+
263 panchromatic images using 10-12 GCP per photograph. After co-registration, $RMSE_{x,y}$ values
264 not exceeding 6.5 m were achieved for both ASTER and Landsat. ASTER 2001 and 2010
265 images were used to map retreat of glacier termini on Mt. Elbrus to make the retreat rates
266 comparable with the rest of the data set.

267 A change in glacier terminus position can be understood as a length measurement along a
268 central flow line (e.g. Stokes et al., 2006). However, changes in position of glacier termini are
269 not uniform along their margin. To account for this, five measurements were taken across the
270 width of each glacier terminus along flow lines and an average value was calculated in line with
271 similar studies (e.g. Hall et al., 2003; Koblet et al., 2010; Bhambri et al., 2012). The uncertainty
272 in terminus recession was calculated as a combination of the maximum $RMSE_{x,y}$ of image co-
273 registration (8.1 m and 6.5 m for 2001-2010 and 1987-2001 periods in the central sector and 8.3

274 m and 6.5 m in the western sector) and a half of pixel size of the satellite images (7.5 m)
275 resulting in total errors of ± 11.0 m and ± 9.9 m for the two assessment periods for the central
276 sector and ± 11.2 and ± 9.9 m for the western sector.

277

278 **3.4 Meteorological data**

279 There are two high-altitude meteorological stations with continuing observations in the study
280 area, Terskol in the central MCR (43.26°N; 42.51°E; 2141 m a.s.l.) and Klukhorskyi Pereval
281 (Path) in the western sector (43°15'8"N; 41°49'39"E; 2037 m a.s.l.). Continuous records from
282 these stations are available from 1951 and 1960, respectively. Their monthly air temperature and
283 precipitation records were used to characterise climatic variations in the Baksan, Malka and
284 Kuban catchments on the northern slope. Continuous observations from the high-altitude regions
285 of the Inguri and Kodori catchments are not available. Records from Abastumani station, located
286 south of the study region (41.77°N; 42.83°E; 1265 m a.s.l.), available for the 1951-2005 period,
287 were used to characterise changes on the southern slope of the central MCR.

288

289 **4 Results**

290 **4.1 The Main Caucasus Ridge**

291 **4.1.1. Area change**

292 In total, 478 glaciers located in the central and western MCR lost 13.4 km² or 4.7 \pm 2.1% of their
293 map area between 2000/2001 and 2010 (Table 2). Glaciers in the central MCR lost 8.5 km² or
294 5.0 \pm 2.4% of their area (0.6% a⁻¹); in the western sector, the area declined by 4.9 km² or
295 4.1 \pm 2.7% (0.4% a⁻¹). Overall, the differences between the slopes and sectors were small and
296 within uncertainty of the measurements. The greatest loss was observed on the southern slope in

297 the central MCR where glaciers lost $5.6\pm 2.5\%$ of their combined map area in 9 years and the
298 lowest on the southern slope of the western MCR where glaciers lost $3.8\pm 2.7\%$ although we note
299 that these differences are within the uncertainty margin. Of all glaciers in the sample, twenty lost
300 over 20% of their 2000/2001 areas and forty one glaciers lost between 10% and 20%.

301 There are two compound-basin valley glaciers in the sample, both located in the Inguri
302 catchment. They experienced a slower recession than glaciers of other types (Table 3), losing
303 $2.80\pm 1.8\%$ of their areas. Both glaciers are among the largest in the sample with 2001 areas of
304 31.4 km^2 (Lekzyri; the third largest glacier in the Caucasus and the largest in the sample) and 9.4
305 km^2 (Chalaati). There are no statistically significant differences in area loss between other types
306 of glaciers for the MCR as a whole, however, some differences between the northern and
307 southern slopes and the sectors were just outside the uncertainty margin (Table 3). Thus the
308 relative area loss by valley glaciers in the central sector of the MCR was twice as high as in the
309 western sector and valley glaciers located on the southern slope of the central MCR lost the
310 highest proportion of their map area in the whole sample. The valley glaciers in the central MCR
311 are larger than in the west and while their higher absolute loss (4.6 km^2 against 1.9 km^2 in the
312 west) is expected, a higher relative loss is not in line with trends observed in other regions and is
313 likely to result from lower precipitation in the central MCR in comparison with the west (see Fig.
314 6).

315 In contrast to other glacierized regions (e.g. Paul et al., 2004; Citterio et al., 2007) and in rare
316 agreement with DeBeer and Sharp (2007), the smallest glaciers exhibited the lowest relative
317 change in the central MCR. Thus glaciers with 2001 map areas of $0.02\text{-}0.1 \text{ km}^2$ lost in total
318 $0.9\pm 3.0\%$ of their combined area; this loss resulted from a 33% reduction in area of a single
319 glacier while another 36 did not exhibit measurable change. Glaciers within the $0.1\text{-}1.0 \text{ km}^2$ and

320 1.0-5.0 km² categories lost 5.2±2.2%. Those larger than 5 km² lost 3.7%. In the western MCR,
321 the difference was less marked and within the uncertainty margin. Glaciers with 2000 map area
322 of 0.02-0.1 km² lost in total 3.9% of their combined area which is higher than in the central
323 sector despite higher precipitation. Glaciers with 2000/2001 map areas of 0.1-1.0 km² and 1.0 -
324 3.0 km² lost 4.7% and 3.2% respectively.

325

326 **4.2 Mt. Elbrus**

327 Glaciers located on Mt. Elbrus lost 5.8±1.4 km² or 4.9±1.2% (0.4 % a⁻¹) of their combined
328 area between 1999 and 2012. Their recession rate is comparable with glacier area loss in the
329 MCR despite the higher elevation and larger accumulation to ablation area ratios (AAR) of the
330 Elbrus glaciers (Table 4; Fig. 4). A characteristic feature of glacier recession on Mt. Elbrus is the
331 expansion of nunataks, exposed rocks and separation of sections of glaciers in the ablation zone
332 below approximately 4000 m a.s.l. Nunataks and exposed rocks were not accounted for in the
333 previous measurements (e.g. Zolotarev and Kharkovets 2012) although their combined area was
334 4.1 km² or 3.5% of the Elbrus glaciated massif in 1999. In 2012, their combined area was 3.7
335 km². However, the reduction in their absolute area is misleading because in the lower parts of the
336 ablation zone they merged with the surrounding rocks. Calculated relatively to the boundaries of
337 glaciated area as in 1999, the area of ‘nunataks’ and exposed rocks was approximately 6 km².
338 Fig. 5 illustrates the expansion of exposed rocks on the southern slope of Mt. Elbrus including
339 Bolshoi Azau, Malyi Azau and Garabashi glaciers. Two areas of exposed rocks expanded
340 considerably over the last decade, e.g. between Bolshoi Azau and Malyi Azau glaciers (Fig. 5 b).
341 In all, eight small ice bodies with a total area of 0.3 km² had separated from the main glacier
342 massif by 2012.

343 Changes in areas of individual glaciers are summarized in Table 4. In absolute terms, the
344 Bolshoi Azau and Dzhikiugankez glaciers experienced the largest recession losing 1.2 km² and
345 1.9 km². In relative terms, two small hanging glaciers (N 311 and 312) located west of the
346 Bolshoi Azau glacier (Fig. 4 and 5) lost the largest proportion of their map area, 15.2% and
347 15.4% each, although in absolute terms the loss is small at 0.1 km². The larger glaciers lost
348 between 1% and 7.4%. Among the larger glaciers, the highest relative loss characterised
349 Dzhikiugankez ice plateau, Garabashi and Irikchat glaciers. The area losses of Glacier N 317
350 (Fig. 4), which terminates over a cliff at approximately 4400 m a.s.l., and Glacier N 319 were not
351 detectable. The difference in area loss between glaciers with different aspect is close to the
352 accuracy of measurements for glaciers with southern (5.6%), eastern (5.0%) and northern (4.3%)
353 aspect. The three glaciers with western aspect lost 2.5% of their areas.

354

355 **4.3 Teminus retreat**

356 Data on retreat of glacier termini are summarised in Table 5. Across the region, terminus retreat
357 increased from the 1987-2000/2001 period to the 2000/2001-2010 period by the factor 2.5 – 3.8.
358 The highest recession rates of 11-14 m a⁻¹ were observed in the central MCR and on Mt. Elbrus,
359 where glaciers are larger, with the strongest acceleration on the southern slope of the MCR. The
360 largest total retreat was exhibited by the Bolshoi Azau glacier, located on Mt. Elbrus, which is
361 the second largest glacier in the sample. This glacier lost 500 m, retreating at a steady rate of 22
362 m a⁻¹. The largest glacier in the sample, Lekzyri, located on the southern slope, lost 40 m and 200
363 m (2.5% of its 2001 length) in the two periods respectively. Two benchmark glaciers, Djankuat
364 and Garabashi, retreated by 185 m and 170 m in total. Retreat of glacier termini in the western

365 sector was more subdued, especially on the southern slope, where glaciers were receding by 3.2
366 m a⁻¹ in the first decade of the 21st Century.

367

368 **4.4 Climatic variability**

369 The observed glacier recession is consistent with increasing air temperature of the ablation
370 season (June-July-August; JJA) registered in both central and western MCR (Fig. 6 a). In the
371 central MCR, at Terskol station, the average JJA temperatures in 1987-2001 and 2001-2010 were
372 11.6°C and 11.7°C respectively, exceeding the mean JJA temperature of 10.9°C registered
373 between 1960 and 1986. Similar trends are observed in the western MCR where the average JJA
374 temperatures at Klukhorskyi Pereval station in 1987-2001 and 2001-2010 were 12.3°C and
375 12.5°C respectively exceeding the 1960-1986 mean JJA temperature of 11.8°C. The JJA
376 temperature record from Abastumani (not shown) is intermittent and terminates in 2005,
377 however, it correlates closely with the Terskol record ($r=0.90$) in the overlapping period and
378 indicates strong climatic warming between the 1980s and 2005. It should be noted, however, that
379 despite the warming observed in the last two decades, the 1951-1960 decade still remains the
380 warmest on record in the central MCR with an average JJA temperature of 12.4°C (Fig. 6a).

381 An increase in the accumulation season (October-April) precipitation, statistically significant
382 at 95% confidence level, was registered at both Terskol and Klukhorskyi Pereval in the 1987-
383 2010 period, when the averages of 538 mm and 1173 mm exceeded the 1960-1986 averages of
384 427 mm and 1037 mm by 26% and 13% respectively (Fig. 6b). At Terskol, a positive linear trend
385 for the 1951-2011 period was statistically significant. It indicated a 35 mm increase in the
386 accumulation season precipitation per decade and explained 19% of the total variance in the data
387 set. By contrast, the accumulation season precipitation did not change at Abastumani in 1987-

388 2005 in comparison with 1960-1986. By 2005, a statistically significant change in precipitation
389 had already occurred on the northern slope at both stations.

390

391 **5 Discussion**

392 In the central and western sectors of the MCR and on Mt. Elbrus, the measured glacier map area
393 reduction in the first decade of the 21st Century of $4.7 \pm 2.1\%$ exceeded uncertainties associated
394 with image co-registration, delineation of glacier outlines and presence of debris cover (Table 2).

395 The total mapping error for ASTER imagery was estimated as $\pm 2.4\%$ and $\pm 2.7\%$ for the central
396 and western MCR glaciers respectively and $\pm 1.2\%$ for Mt. Elbrus. This is lower than errors
397 resulting from the use of Landsat imagery (e.g. Paul et al., 2004; Stokes et al., 2006; Bhambri et
398 al., 2011) and similar to or slightly lower than in other studies utilising ASTER imagery (e.g.
399 Bhambri et al., 2011; Shahgedanova et al., 2012). The latter difference is due to the limited
400 extent of debris cover, size distribution and morphology of glaciers in the sample. The supra-
401 glacial debris cover significantly reduces the accuracy of glacier mapping (e.g. Racoviteanu et
402 al., 2008; Bhambri et al., 2011; Paul et al., 2013). However, in the Caucasus the extent of supra-
403 glacial debris is relatively small, typically accounting for 3-25% of individual glacier areas
404 (Stokes et al., 2007) although there are exceptions such as Donguz-Orun. Importantly, debris-
405 covered glaciers have clearly identifiable snout margins. Larger errors arise when mapping very
406 small glaciers with map areas below 0.1 km^2 (e.g. Shahgedanova et al., 2012), however, only
407 20% of the glaciers in the assessed sample were smaller than 0.1 km^2 in 2001 and these were
408 mostly cirque glaciers with clearly defined margins.

409 Although differences between glacier wastage in different sectors of the MCR are close to the
410 measurement uncertainty, it is possible to suggest that glaciers located on the southern slope of

411 the central MCR lost a higher proportion of their area than glaciers in other regions of the
412 Caucasus, $5.6 \pm 2.5\%$ (Table 2). The valley glaciers lost even higher proportion, 7.4% (Table 3)
413 which is the highest value in the whole sample. A higher rate of glacier wastage in the south is
414 consistent with the observed trends in precipitation. Negative precipitation anomalies were
415 observed in on the southern slope in the 1990s. In the 2000s, precipitation anomalies were
416 positive but lower than in the north (Fig. 6b). These trends are consistent with the impacts of
417 NAO on precipitation in southern Europe and westernmost regions of Asia (Marshall et al.,
418 2001). By contrast, glaciers on the southern slope of the western MCR lost 3.8% of their area
419 which is the lowest wastage in the region (Table 2) with valley glaciers losing 2.9% in the north
420 and 3.6% in the south (Table 3). It is likely that high accumulation season precipitation,
421 exceeding that in the central MCR by the factor of 2-3 (Volodicheva, 2002) and persistent
422 positive precipitation anomalies observed since the mid-1990s, slowed down glacier retreat in
423 the western MCR.

424 The glaciers on Mt. Elbrus lost the same percentage of their combined area as glaciers in the
425 central MCR despite the higher AAR (Table 2). We calculated the area reduction as $4.9 \pm 1.2\%$
426 with a rate of decrease of $0.4\% \text{ a}^{-1}$ between 1999 and 2012. Zolotarev and Kharkovets (2012),
427 who assessed glacier area change on Mt. Elbrus in the 1997-2007 period using aerial
428 photography from 1997 and Cartosat-1 imagery with spatial resolution of 2.5 m, reported an
429 overall 3.8% area loss. The difference between the two assessments is small and, in addition to
430 measurement uncertainties, reflects slightly different periods of assessments and interpretation of
431 nunataks and bare rocks as glacierised area by Zolotarev and Kharkovets (2012). Holobaca
432 (2013) reported area change of 9.1% between 1985 and 2007 ($0.4\% \text{ a}^{-1}$) from Landsat TM
433 imagery which is the same as in our assessment.

434 The average rate of terminus recession of valley glaciers doubled in the north and more than
435 tripled in the south in the 21st Century in comparison with 1987-2001. Using the approximation
436 by Johansson et al. (1989) based on a ratio between glacier depth at ELA and mass balance near
437 the glacier terminus, dynamic response times of Djankuat and Garabashi glaciers are estimated
438 as 12-15 and 17-18 years respectively. The observed glacier recession and its acceleration in the
439 last decade detected from the changes in the rate of snout retreat are consistent with the positive
440 trend in summer air temperatures since the 1990s. Strong positive anomalies of 2°C in 2006 and
441 2010 (Fig. 6a) contributed to enhanced glacier melt (Fig. 7). The exceptional heat wave which
442 developed over European Russia in July-August 2010 (Grumm, 2011) was as detrimental for the
443 state of the Caucasus glaciers as the 2003 West European heat wave for the glaciers in the Alps
444 (Haeberli et al., 2007). The mass balance records for Garabashi show that in the summer of 2010
445 alone, the glacier lost 2.52 m w.e., close to the record loss of 2.58 m w.e. in the El Niño year of
446 1998 and nearly twice the long-term average (1984 to current). A strong decline in cumulative
447 mass balance (Fig. 7) occurred after 1998 despite a 20% increase in precipitation (Fig. 6b) north
448 of MCR (WGMS, 2013).

449 Glacier shrinkage in the Caucasus appears to be slower than in the European Alps. Paul et al.
450 (2004) reported 18% (1.3% a⁻¹) glacier shrinkage in the Swiss Alps in the 1985-1999 period.
451 Fischer et al. (2014) reported 33% (1.1% a⁻¹) and 11% (1.3 % a⁻¹) shrinkage for the eastern Swiss
452 Alps for the 1973-2003 and 2003-2009 periods respectively. Maragno et al. (2009) reported
453 5.5% (1.4% a⁻¹) shrinkage in 1999-2003 and even stronger shrinkage of 11% or 2.8% a⁻¹ was
454 reported by Diolaiuti et al. (2011) for the Italian Alps. The heat wave of 2003 had a strong
455 impact on glacier wastage in the European Alps (Haeberli et al., 2007), however, even prior to
456 this extreme event, glacier wastage rates in the Alps exceeded those of 0.4-0.6% a⁻¹ that we

457 report for the Caucasus. Another important difference is contribution of small glaciers to the
458 overall reduction of glacierized area. Thus in the Swiss and Lombardy Alps, glaciers with
459 individual areas less than 1 km² contributed about 40% and 58% of total area loss while
460 accounting for only 15% and 30% of glacierized area respectively (Paul et al., 2004; Citterio et
461 al., 2007). Glaciers of the same size category occupied 22.3% of the glacierized area in MCR and
462 contributed 7.3% of area loss. Topographic effect and geographical distribution of glaciers are
463 the most likely explanation. Larger glaciers are valley glaciers, whose tongues open to sunlight
464 exhibit a stronger retreat. Smaller glaciers are mostly cirque glaciers whose recession is restricted
465 by topography and shading provided by the cirque walls. Slower wastage of small cirque glaciers
466 due to the shading effect was reported by Shahgedanova et al. (2012) for the Polar Urals. In the
467 central MCR, the difference is more pronounced than in the western sector because larger valley
468 glaciers are located on the southern slope where negative precipitation anomalies contributed to
469 stronger glacier retreat (Table 3).

470

471 **6 Conclusions**

472 To conclude, (i) the Caucasus glaciers lost $4.7 \pm 2.1\%$ of their total area between 2000 and
473 2010/2012 and the estimate exceeds the uncertainty of the measurements; (ii) glaciers of Mt.
474 Elbrus lost a similar proportion of their area to that lost by the glaciers located in the MCR
475 despite higher elevation and large AAR; (iii) the largest wastage occurred on the southern slope
476 of the central sector in line with precipitation anomalies; (iv) the retreat of glacier termini
477 accelerated in the first decade of the 21st century in comparison with the end of the 20th century.

478

479 **Acknowledgements**

480 We are grateful to the reviewers, Prof. Gogley and Dr. Bhambri, and to the editor, Dr. Bolch, for
481 the very detailed comments which helped to improve the paper.

482

483 **References**

484 Andreassen, L.M., Paul, F., Kääb, A. and Hausberg, J.E.: Landsat-derived glacier inventory for
485 Jotunheimen, Norway, and deduced glacier changes since the 1930s. *The Cryosphere*, 2, 131-
486 145, doi:10.5194/tc-2-131-2008, 2008.

487 Arendt, A. et al. (79 authors): Randolph Glacier Inventory [v2.0]: A Dataset of Global Glacier
488 Outlines, Boulder, Colorado, Digital Media, <http://www.glims.org/RGI/randolph.html> (last
489 access: 7 July 2014), 2012.

490 Bhambri, R., Bolch, T., Chaujar, R.K. and Kulshreshtha S.C.: Glacier changes in the Garhwal
491 Himalaya, India, from 1968 to 2006 based on remote sensing. *J. Glaciol.*, 57 (203), 543-556,
492 2011.

493 Bhambri, R., Bolch, T., and Chaujar, R.K.: Frontal recession of Gangotri Glacier, Garhwal
494 Himalayas, from 1965-2006, measured through high resolution remote sensing data. *Current*
495 *Science*, 102, 489-494, 2012.

496 Bolch, T., Buchroithner, M.F., Pieczonka, T., Kunert, A.: Planimetric and volumetric glacier
497 changes in the Khumbu Himalaya 1962 – 2005 using Corona and ASTER data. *J. Glaciol.*,
498 54(187), 562-600, 2008.

499 Bolch, T., Menounos, B. and Wheate, R.: Landsat-based inventory of glaciers in western
500 Canada, 1985–2005, *Rem. Sens. Environ.*, 114, 127–137, 2010.

501 Borovik, E.S. and Kravtsova, V.I.: Catalogue of Glaciers of the USSR, Gidrometeoizdat,
502 Leningrad, Vol. 8, Part 5, Basins of the Malka and the Baksan Rivers, 86 pp., 1970 (in
503 Russian).

504 Bushueva, I.S. and Solomina, O.N.: Kolebaniya lednika Kashkatash v XVII-XXI vv. po
505 kartograficheskim, dendrohronologicheskim i lichonometriceskim dannym (Fluctuations of
506 Kashakataash Glacier in XVII-XXI centuries according to cartographic, dendrochronological
507 and lichonometric data). *Led i Sneg (Ice and Snow)*, 2 (118), 121-130, 2012 (in Russian).

508 Church, J.A., White, N.J., Konikow, L.K., Domingues, C. M. ., Cogley, J. G., Rignot, E.,
509 Gregory, J. M., van den Broeke, M. R., Monaghan, A. J. and Velicogna, I.: Revisiting the
510 Earths sea-level and energy budgets from 1961 to 2008, *Geophys. Res. Lett.*, L18601,
511 doi:10.1029/2011GL048794, 2012.

512 Citterio, M., Diolaiuti, G., Smiraglia, C., D'Agata, C., Carnielli, T., Stella, G. and Siletto, G.B.:
513 The fluctuations of Italian glaciers during the last century: A contribution to knowledge about
514 Alpine glacier changes. *Geogr. Annal. A*, 89 A, 167-184, 2007.

515 DeBeer, C.M. and Sharp, M.J.: Recent changes in glacier area and volume within the Southern
516 Canadian Cordillera, *Ann. Glaciol.*, 46 (1), 215–221, 2007.

517 Diolaiuti, D., Maragno, D., D'Agata, C., Smiraglia, C., and Bocchiola, D.: Glacier retreat and
518 climate change: Documenting the last 50 years of Alpine glacier history from area and
519 geometry changes of Dosde Piazzis glaciers (Lombardy Alps, Italy). *Prog. Phys. Geog.*, 35,
520 161-182, 2011.

521 Dolgova, E.A., Matskovsky, V.V., Solomina, O.N., Rototaeva, O.V., Nosenko, G.A., and
522 Khmelevsky, I.F.: Reconstructing mass balance of Garabashi Glacier (1800-2005) using
523 dendrochronological data, *Led i Sneg (Ice and Snow)*, 1 (121), 34-43, 2013 (in Russian).

524 Dyurgerov, M.B. and Meier, M.F: Twentieth century climate change: evidence from small
525 glaciers. *P. Nat. Acad. Sci. USA*, 97, 1406-1411, 2000.

526 Frey, H., Paul, F. and Strozzi, T.: Compilation of a glacier inventory for the western Himalayas
527 from satellite data: methods, challenges, and results. *Rem. Sens. Environ.*, 124: 832-843, 2012.

528 Fischer, M., Huss, M., Barboux, C., and Hoelzle, M.: The new Swiss Glacier Inventory
529 SGI2010: Relevance of using high-resolution source data in areas dominated by very small
530 glaciers. *Arct. Antarct. Alp. Res.*, 46(4), 933-945, 2014.

531 Granshaw, F.D. and Fountain, A.G.: Glacier change (1958-1998) in the North Cascades National
532 Park Complex, Washington, USA. *J. Glaciol.*, 52 (177), 251-256, 2006.

533 Grumm, R.H.: The Central European and Russian heat event of July-August 2010. *B. Am.*
534 *Meteorol. Soc.*, 92: 1285-1296, 2011.

535 Haerberli, W., Hoelzle, M., Paul, F. and Zemp, M.: Integrated monitoring of mountain glaciers as
536 key indicators of global climate change: the European Alps. *Ann. Glaciol.*, 46 (1), 150-160,
537 2007.

538 Hall, D.K., Bayr, K.J., Schöner, W., Bindschadler, R.A., and Chein, J.Y.L.: Consideration of the
539 errors inherent in mapping historical glacier positions in Austria from the ground and space
540 (1983-2001), *Remote Sens. Environ.*, 86, 566-577, 2003.

541 Hoelzle, M., Haerberli, W., Dischl, M. and Peschke, W.: Secular glacier mass balances derived
542 from cumulative glacier length changes. *Glob. Plan. Change*, 36, 295-306, 2003.

543 Holobaca, I-H: Glacier Mapper – a new method designed to assess change in mountain glaciers,
544 *Int. J. Rem. Sens.*, 34 (23), 8475-8490, 2013.

545 IPCC 2013: Climate Change 2013: The Physical Science Basis. Contribution of Working Group
546 I to the Fifth Assessment Report of the Intergovernmental Panel on Climate Change, edited by:
547 Stoker, T.F., Qin, D., Plattner, G-K., Tignor, M., Allen, S.K., Boschung, J., Nauels, A., Xia,
548 Y., Bex, V., and Midgley, P.M. Cambridge University Press, Cambridge, 1535 pp.

549 Jóhannesson, T., Raymond, C. and Waddington, E.: Time-scale for adjustment of glaciers to
550 changes in mass balance. *J. Glaciol.*, 35 (121), 355– 369, 1989.

551 Keinholz, C., R. Hock, and A.A. Arendt: A new semi-automatic approach for dividing glacier
552 complexes into individual glaciers. *J. Glaciol.*, 59 (217), 925-937, 2013.

553 Koblet, T., Gartner-Roer, I., Zemp, M., Jansson, P., Thee, P., Haeberli, W. and Holmlund, P.:
554 Reanalysis of multi-temporal aerial images of Storglaciaren, Sweden (1959–99) – Part 1:
555 Determination of length, area, and volume changes. *The Cryosphere*, 4, 333-343,
556 doi:10.5194/tc-15 4-333-2010,2010.

557 Kutuzov S., Lavrentiev, I.I., Macheret, Yu. Ya. and Petrakov, D.A.: Changes of Marukh Glacier
558 from 1945 to 2011 *Led i Sneg (Ice and Snow)*, 1 (117), 123-128, 2012 (in Russian).

559 Lang, H.R., and Welch, R.: ATBD-AST-08 Algorithm theoretical basis document for ASTER
560 digital elevation models (Standard product AST14),
561 http://eospsso.gsfc.nasa.gov/eos_homepage/for_scientists/atbd/docs/ASTER/atbd-ast-14.pdf,
562 (last access: 7 July 2014), 1999.

563 Leclercq, P.W. and Oerlemans, J.: Global and hemispheric temperature reconstruction from
564 glacier length fluctuations. *Clim. Dyn.*, 38: 1065-79, 2012.

565 Leclercq, P.W., Oerlemans, J., Basagic, H. J., Bushueva, I., Cook, A. J., and Le Bris, R.: A data
566 set of worldwide glacier length fluctuations, *The Cryosphere*, 8, 659-672, doi:10.5194/tc-8-
567 659-2014, 2014.

568 Maragno, D., Diolaiuti, G., D'Agata, C., Mihalcea, C., Bocchiola, D., Janetti, E.B., Riccardi, A.
569 and Smiraglia, C.: New evidence from Italy (Adamello Group, Lombardy) for analyzing the
570 ongoing decline of Alpine glaciers. *Geograf. Fis. Dinam. Quaternaria*, 32, 31-39, 2009.

571 Marshall, J., Kushnir, Y., Battisti, D., Chang, P., Czaja, A., Dickson, R., Hurrell, J., McCartney,
572 M., Saravanan, R., and Visbeck, M.: North Atlantic climate variability: phenomena, impacts
573 and mechanisms. *Int. J. Climatol.*, 21, 1863-1898, 2001.

574 Maruashvili, L.I., Kurdgelaidze, G.M. and Lashkhi, T.A.: Catalogue of Glaciers of the USSR,
575 Vol. 9, Parts 2-6, Basin of the Kodori and Inguri Rivers, Gidrometeoizdat, Leningrad, 86 pp.,
576 1975 (in Russian).

577 Meyer, D., Tachikawa, T., Kaku, M., Iwasaki, A., Gesch, D., Oimoen, M., Zhang, Z., Danielson,
578 J., Krieger, T., Curtis, B., Haase, J., Abrams, M., Crippen, R., and Carabajal, C.: ASTER
579 Global Digital Elevation Model Version 2 – Summary of Validation Results. NASA Land
580 Processes Distributed Active Archive Center, online report [http://www.jspacesystems.or.jp/
581 ersdac/GDEM/ver2Validation/Summary_GDEM2_validation_report_final.pdf](http://www.jspacesystems.or.jp/ersdac/GDEM/ver2Validation/Summary_GDEM2_validation_report_final.pdf) (last access: 7
582 July 2014), 26 pp., 2011.

583 Nakano, K., Zhang, Y., Shibuo, Y., Yabuki, H. and Hirabayashi, Y.: A monitoring system for
584 mountain glaciers and ice caps using 30 meter resolution satellite data. *Hydrol. Res. Let.*, 7(3),
585 73–78, 2013.

586 Panov, V.D.: *Evolyutsiya sovremennogo oledeneniya Kavkaza (Evolution of the Contemporary
587 Glaciation in the Caucasus)*, Gidrometeoizdat. St. Petersburg, 432 pp, 1993 (in Russian).

588 Panov, V.D. and Kravtsova, V.I.: Catalogue of Glaciers of the USSR, Vol. 8, Parts 1-4, Basin of
589 the Kuban River, Girdometeoizdat, Leningrad, 145 pp., 1967 (in Russian).

590 Paul, F., Kääb, A., Maisch, M., Kellenberger, T. and Haeberli, W.: The new remote-sensing-
591 derived Swiss glacier inventory: I. Methods. *Ann. Glaciol.*, 34, 355–361, 2002.

592 Paul, F., Kääb, A., Maisch, M., Kellenberger, T. and Haeberli, W.: Rapid disintegration of
593 Alpine glaciers observed with satellite data. *Geophys. Res. Lett.*, 31(21), L21402,
594 10.1029/2004GL020816, 2004.

595 Paul, F. and Andreassen, L.M.: A new glacier inventory for the Svartisen region, Norway, from
596 Landsat ETM+ data: challenges and change assessment. *J. Glaciol.*, 55 (192), 607-618, 2009.

597 Paul, F., Barry, R., Cogley, G., Frey, H., Haeberli, W., Ohmura, A., Ommanney, S., Raup, B.,
598 Rivera, A., and Zemp, M.: Recommendations for the compilation of glacier inventory data
599 from digital sources, *Ann. Glaciol.*, 50 (53), 119-126, 2009.

600 Paul, F., Barrand, N.E., Baumann, S., Berthier, E., Bolch, T., Casey, K., Frey, H., Joshi, S.P.,
601 Konovalov, V., Le Bris, R., Mölg, N., Nosenko, G., Nuth, C., Pope, A., Racoviteanu, A.,
602 Rastner, P., Raup, B., Scharrer, K., Steffen, S. and Winsvold, S: On the accuracy of glacier
603 outlines derived from remote-sensing data, *Ann. Glaciol.*, 54(63), 171-182, 2013.

604 Popovnin, V.V.: Pole akkumulyatsii gornogo lednika (Accumulation Zone of a Mountain
605 Glacier) *Mater. Glyatsiol. Issled.*, (Data Glaciol. Res.), 88, 27– 40, 2000 (in Russian).

606 Popovnin, V.V. and Petrakov, D.A.: Lednik Djankuat za poslednie 34 goda, 1967/68-2000/01
607 (Djankuat Glacier in the last 34 years, 1967/68-2000/01). *Mater. Glyatsiol. Issled.*, (Data
608 Glaciol. Res.), 98, 167-175, 2005 (in Russian).

609 Rototaeva, O. Data on surging glaciers in the Northern Caucasus, in: *Oledenenie Severnoi i*
610 *Tsentralnoi Evrazii v Sovremennuyu Epohu (Glaciation in Northern and Central Eurasia at*
611 *Present Time)*, edited by: Kotlyakov, V.M., Nauka Publishers, Moscow, 215-223, 2006 (in
612 Russian).

613 Rototaeva, O., Nosenko, G., Tarasova, L., and Khmelevsky, I.: Caucasus, in *Oledenenie*
614 *Severnoi i Tsentralnoi Evrazii v Sovremennuyu Epohu (Glaciation in Northern and Central*

615 Eurasia at Present Time), edited by: Kotlyakov, V.M., Nauka Publishers, Moscow, 141-162,
616 2006 (in Russian).

617 Racoviteanu, A.E., Williams, M.W. and Barry, R.G.: Optical Remote Sensing of Glacier
618 Characteristics: A Review with Focus on the Himalaya. *Sensors*, 8, 3355-3383, 2008.

619 Schiefer, E., B. Menounos, and Wheate, R.D.: An inventory and morphometric analysis of British
620 Columbia glaciers, Canada, *J. Glaciol.*, 54 (186), 551-560, 2008.

621 Shahgedanova, M., Stokes, C.R., Gurney, S.D. and Popovnin, V.V.: Interactions between mass
622 balance, atmospheric circulation and recent climate change on the Djankuat glacier, Caucasus
623 Mountains, Russia, *J. Geophys. Res.–Atm.*, 110 (D4), D04108, 10.1029/2004JD005213, 2005.

624 Shahgedanova, M., Popovnin, V., Aleynikov, A., Petrakov, D. and Stokes, C.R.: Long-term
625 change, inter-annual, and intra-seasonal variability in climate and glacier mass balance in the
626 central Greater Caucasus, Russia, *Ann. Glaciol.*, 46 (1), 355-361, 2007.

627 Shahgedanova, M., Nosenko, G., Bushueva, I. and Ivanov, M.: Changes in area and geodetic
628 mass balance of small glaciers, Polar Urals, Russia, 1950-2008. *J. Glaciol.*, 58 (211), 953-964,
629 2012.

630 Stokes, C.R., Gurney, S.D., Shahgedanova, M. and Popovnin, V.V.: Late-20th-century changes
631 in glacier extent in the Caucasus Mountains, Russia/Georgia, *J. Glaciol.*, 52 (176): 99-109,
632 2006.

633 Stokes, C.R., Popovnin, V.V., Aleynikov, A. and Shahgedanova, M.: Recent glacier retreat in the
634 Caucasus Mountains, Russia, and associated changes in supraglacial debris cover and
635 supra/proglacial lake development. *Ann. Glaciol.*, 46 (1), 196-203, 2007.

636 Svoboda, F. and Paul, F.: A new glacier inventory on southern Baffin Island, Canada, from ASTER data:
637 I. Applied methods, challenges and solutions, *Ann. Glaciol.*, 50 (53), 11-21, 2009.

638 Volodicheva, N.: The Caucasus, in *The Physical Geography of Northern Eurasia*, edited by:
639 Shahgedanova, M., 350– 376, Oxford University Press, Oxford, 2002.

640 WGMS: *Glacier Mass Balance Bulletin No. 12 (2010-2011)* and earlier issues edited by: Zemp,
641 M., Nussbaumer, S.U., Gärtner-Roer, I.I., Hoelzle, M., Paul, F. and Haerberli, W., ICSU(WDS)
642 / IUGG (IACS) / UNEP / WMO. World Glacier Monitoring Service, Zurich, Switzerland, 106
643 pp., 2013.

644 Yefremov, Yu.V., Panov, V.D., Lurie, P.M., Iliychev, Yu.S., Panova, S.V., and Lutkov, D.A.:
645 Orografiya, oledenenie, klimat Bolshogo Kavkaza (Orography, Glaciation and Climate of the
646 Greater Caucasus). Kubanskyi State University Press, Krasnodar, 337 pp., 2007 (in Russian).

647 Zemp, M., Hoelzle, M. and Haerberli, W.: Six decades of glacier mass-balance observations: a
648 review of the worldwide monitoring network. *Ann. Glaciol.*, 50 (50), 101-111, 2009.

649 Zolotarev, E.A. and Kharkovets, E.G.: Oledenenie Elbrusa kontse XX veka (Glaciation of Mt.
650 Elbrus at the end of the 20th Century). *Led i Sneg (Ice and Snow)*, 5 (112), 45-51, 2007 (in
651 Russian).

652 Zolotarev, E.A. and Kharkovets, E.G.: Evolyutsiya oledeneniya Elbrusa posle malogo
653 lednikovogo perioda (Evolution of glaciation on Mt Elbrus after the Little Ice Age). *Led i Sneg*
654 (Ice and Snow), 2 (118), 5-14, 2012 (in Russian).

655

656 Table 1 Details of the imagery used for glacier mapping. Location of catchments are shown
 657 in Fig. 1.

Date	Type of imagery	Region	No of glaciers
6/09/2012	ASTER	Mt. Elbrus 42.96-43.60°N; 42.16-43.05°E	20
18/08/1999	Landsat ETM+ panchromatic; path 171; row 030	Mt. Elbrus 41.14-44.19 °N; 41.94-44.96°E	
15/09/2001	ASTER	Central MCR and Mt. Elbrus for the assessment of recession of glacier termini; 43.05-43.35°N; 42.34-42.83°E	174 in all: 99, 9 and 69 on northern and southern slopes in Baksan, Malka and Inguri catchments respectively
29/09/2010	ASTER		
23/08/2010	ASTER	Western MCR; 43.07-43.43°N; 41.62-42.40°E	304 in all: 147 and 157 on northern (Kuban catchment) and southern (Inguri and Kodori catchments) slopes
12/09/2000	Landsat ETM+ panchromatic; path 171; row 030		
25-26/09/1987	Aerial photographs	43.05-43.35°N; 42.34-42.83°E	28 glaciers: 7 in the Baksan and Adylsu valleys and 14 in the Inguri valley in central MCR; 6 on south-eastern slope of Mt. Elbrus
25-26/09/1987	Aerial photographs	43.07-43.43°N 41.80-42.40°E	17 glaciers in the Kuban, Kodory and Inguri basins in the western MCR

658

659

660 Table 2. Changes in glacierized area.

Region		Combined area (km ²)		Area reduction	
		1999/2000/2001	2010/2012	km ²	%
Central MCR	Total	170.6±2.3	162.1±2.1	8.5±4.1	5.0±2.4
	Northern	73.4±1.1	70.3±1.0	3.1±1.7	4.3±2.3
	Southern	97.2±1.2	91.8±1.1	5.4±2.4	5.6±2.5
Western MCR	Total	118.3±2.1	113.4±2.1	4.9±3.2	4.1±2.7
	Northern	63.2±1.1	60.4±1.1	2.8±1.7	4.4±2.7
	Southern	55.2±1.0	53.1±1.0	2.1±1.5	3.8±2.7
Elbrus		118.4±1.0	112.6±1.0	5.8±1.4	4.9±1.2
Total		407.3±5.4	388.1±5.2	19.2±8.7	4.7±2.1

662 Table 3. Area loss (%) according to glacier type in the Central and Western MCR. Number of
 663 glaciers of each type is given in parentheses. The two compound-valley glaciers located on the
 664 southern slope of the central MCR are not included (see text).

Region	Central			Western			All
Type	North	South	All	North	South	All	
Valley	5.3 (7)	7.4 (25)	6.7	2.9 (19)	3.6 (42)	3.3	5.0
Cirque	4.1 (156)	3.3 (20)	4.0	6.2 (104)	4.4 (85)	5.5	4.6
Hanging	4.5 (4)	0 (3)	4.4	6.6 (23)	0.8 (6)	5.2	5.1
Ice aprons	5.9 (7)	6.8 (15)	6.1	3.5 (11)	4.0 (24)	3.7	5.0

665

666

667 Table 4. Changes in map areas of glaciers located on Mt. Elbrus between 1999 and 2012. All
 668 glaciers are shown in Fig.4.

Number (Fig. 4)	Glacier		Area		Area change	
	Name	WGI ID	1999	2012	km ²	%
1	Ulluchiran	SU4G08005001	11.60±0.08	11.13±0.09	0.50±0.12	4.3±1.0
2	Karachaul	SU4G08005002	7.40±0.04	7.22±0.04	0.22±0.05	3.0±0.7
3	Ullukol and Ullumalienderku	SU4G08005003	4.85±0.04	4.54±0.04	0.31±0.05	6.4±1.0
4	Mikelchiran	SU4G08005005	5.05±0.03	4.86±0.03	0.19±0.04	3.8±0.8
5	Dzhikiugankez	SU4G08005006	26.12±0.17	24.22±0.18	1.90±0.25	7.3±1.0
6	Irikchat	SU4G08005018	1.41±0.03	1.31±0.03	0.10±0.04	7.1±2.8
7	Irik	SU4G08005020	9.18±0.08	8.90±0.08	0.28±0.11	3.1±1.2
8	No 25	SU4G08005025	0.60±0.01	0.56±0.01	0.04±0.01	6.7±1.6
9	Terskol	SU4G08005026	7.99±0.04	7.71±0.03	0.28±0.05	3.5±0.6
10	Garabashi	SU4G08005027	3.26±0.03	3.02±0.03	0.24±0.03	7.4±0.9
11	Malyi Azau	SU4G08005028	8.84±0.07	8.27±0.08	0.57±0.10	6.4±1.1
12	Bolshoy Azau	SU4G08005029	19.70±0.16	18.53±0.16	1.17±0.22	5.9±1.1
13	311	SU4H08004311	0.46±0.01	0.39±0.01	0.07±0.01	15.2±2.2
14	312	SU4H08004312	0.26±0.01	0.22±0.01	0.04±0.01	15.4±3.8
15	313*	SU4H08004313	1.07±0.03	1.05±0.03	0.02±0.04	1.9±3.7
16	Ullukam*	SU4H08004313	0.65±0.03	0.64±0.03	0.01±0.04	1.5±6.0
17	317	SU4H08004317	0.55±0.01	0.55±0.01	0.00±0.01	0.0±1.8
18	Kyukyurtlyu	SU4H08004318	6.92±0.06	6.83±0.06	0.09±0.08	1.3±1.2
19	319	SU4H08004319	0.46±0.02	0.46±0.02	0.00±0.03	0.0±6.5

20	Bityuktyube	SU4H08004320	1.98±0.04	1.90±0.04	0.08±0.06	4.0±3.0
	8 separated ice bodies (Fig. 4)		-	0.30±0.00	-	-
Total			118.4±1.0	112.6±1.0	5.8±1.4**	4.9±1.2

669

670 * Glacier N 313 is a now disconnected part of Ullukam hence the same WGI identification
671 number.

672 ** Including 8 separated ice bodies in 2012

673

674

675 Table 5. Characteristics of glaciers used for measuring snout retreat. The average error terms are

676 ± 9.9 m and ± 11 m for the 1987-2000/2001 and 2000/2001-2010 periods respectively.

Region	Slope	No	Length (km) as in 1987		Length change			
					1987-2000/2001		2000/2001-2010	
			Average	Range	m	m a ⁻¹	m	m a ⁻¹
Central MCR	All	21	4.2	0.8-9.7	52.9	3.8	106.7	11.9
	N	7	4.6	2.8-9.7	77.1	5.5	121.4	13.5
	S	14	4.0	0.8-8.3	40.8	2.9	99.4	11.0
Western MCR	All	17	2.3	0.8-3.6	40.5	3.2	78.5	8.7
	N	13	2.2	0.8-3.6	47.5	3.7	88.6	8.9
	S	4	2.7	1.8-3.3	13.3	1.0	32.7	3.2
Elbrus	SE	6	7.0	2.6-10.2	115.8	8.3	126.7	14.1

677

678

679 **Figure captions**

680 Figure 1. Study area and satellite imagery used for the analysis. The yellow lines show the Black
681 Sea coastline, the MCR, and the catchment boundaries. The catchments are numbered as
682 follows: (1) Kuban; (2) Malka; (3) Baksan; (4) Inguri; and (5) Kodori.

683 Figure 2. Oblique aerial photograph of (a) glaciers on Mt. Elbrus and (b) snout of the Malyi
684 Azau glacier. Note the clearly defined glacier boundaries and a very limited extent of debris
685 cover. Photograph by I.I. Lavrentiev (25 August 2009).

686 Figure 3. Oblique aerial photograph of the Donguz-Orun glacier which has the highest extent of
687 debris cover in the sample. Photograph by I.I. Lavrentiev (25 August 2009).

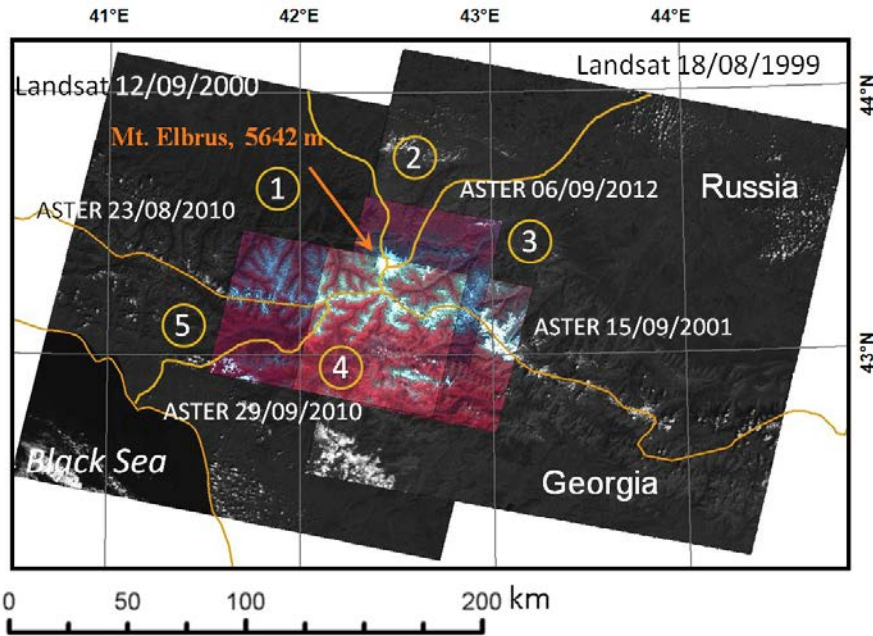
688 Figure 4. Changes in glacierised area of Mt. Elbrus between 1999 and 2012. See Table 4 for the
689 statistics of changes in areas of individual glaciers. The 1999 Landsat ETM+ image (Table 1) is
690 used as background.

691 Figure 5. Expansion of exposed rocks on the southern slope of Mt. Elbrus: (a) 1999 and (b) 2012.
692 Arrows point at the expanded areas of exposed rocks. The 1999 Landsat ETM+ image (Table
693 1) is used as background.

694 Figure 6. (a) JJA temperature and (b) October-April precipitation for Abastumani, Klukhorskyi
695 Pereval and Terskol stations. Horizontal lines show record averages for each station.

696 Figure 7. Cumulative mass balance of Garabashi and Djankuat glaciers (WGMS, 2013;
697 unpublished records from the Institute of Geography, Russian Academy of Science for
698 Garabashi in 2012).

699



700

701

702 Figure 1. Study area and satellite imagery used for the analysis. The yellow lines show the Black

703 Sea coastline, the MCR, and the catchment boundaries. The catchments are numbered as

704 follows: (1) Kuban; (2) Malka; (3) Baksan; (4) Inguri; and (5) Kodori.

705

706



707



708

709 Figure 2. Oblique aerial photograph of (a) glaciers on Mt. Elbrus and (b) snout of the Malyi
710 Azau glacier. Note the clearly defined glacier boundaries and a very limited extent of debris
711 cover. Photograph by I.I. Lavrentiev (25 August 2009).

712

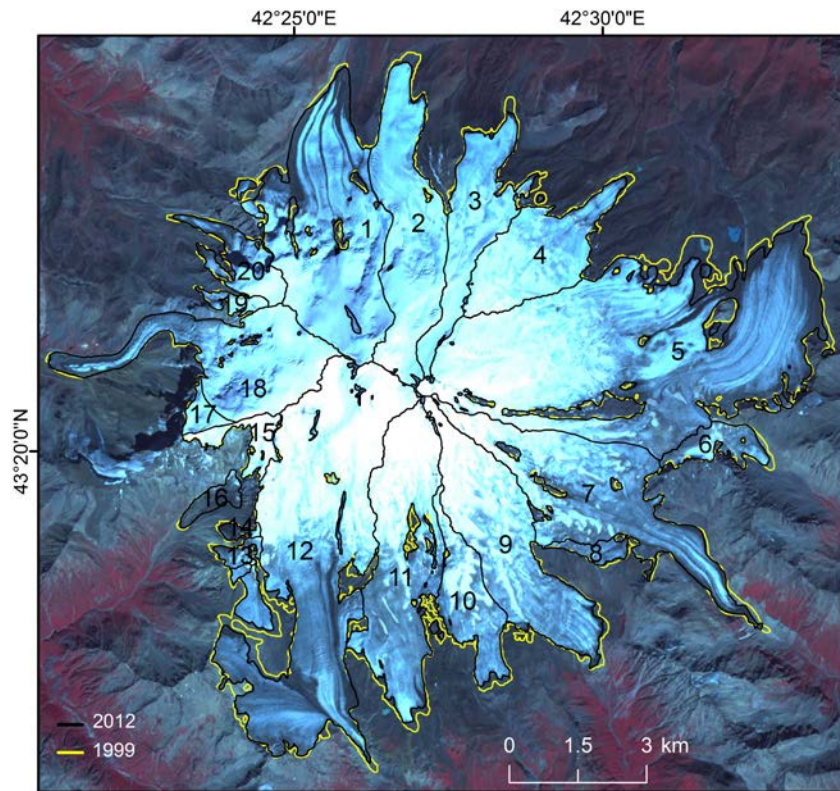


713

714 Figure 3. Oblique aerial photograph of the Donguz-Orun glacier which has the highest extent of

715 debris cover in the sample. Photograph by I.I. Lavrentiev (25 August 2009).

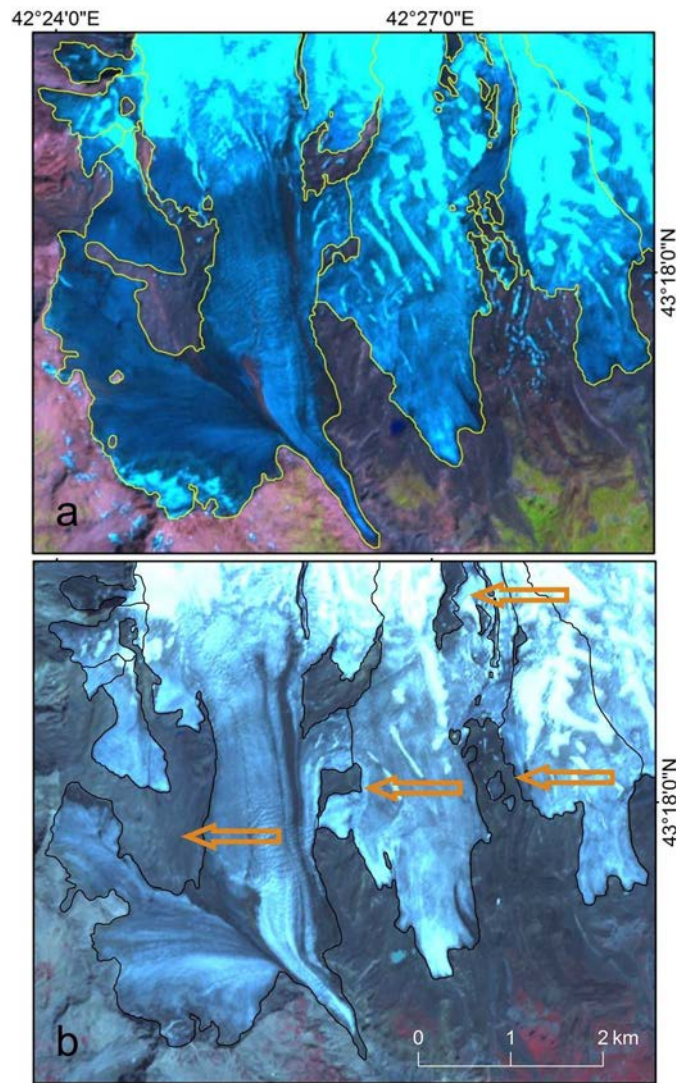
716



717

718 Figure 4. Changes in glacierised area of Mt. Elbrus between 1999 and 2012. See Table 4 for the
719 statistics of changes in areas of individual glaciers. The 1999 Landsat ETM+ image (Table 1) is
720 used as background.

721



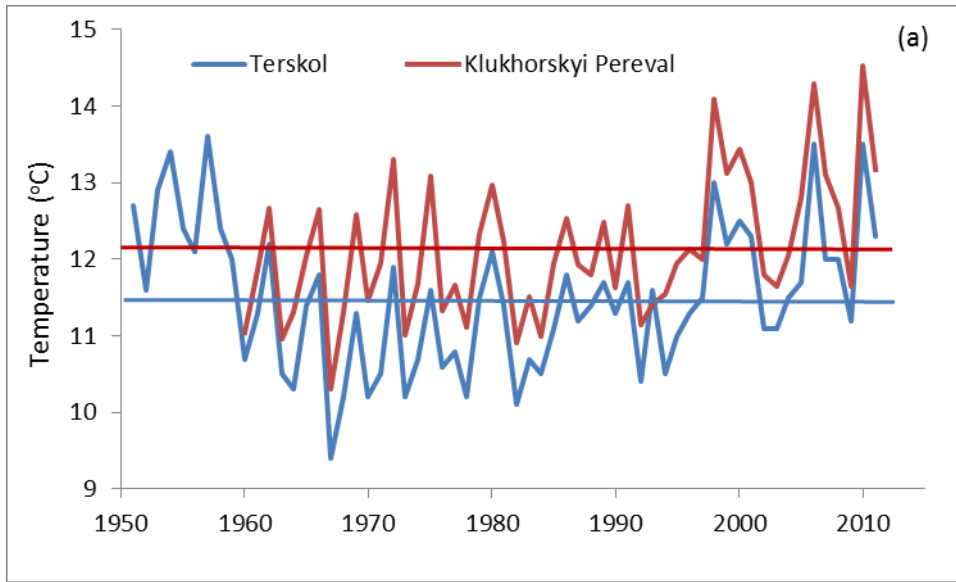
722

723

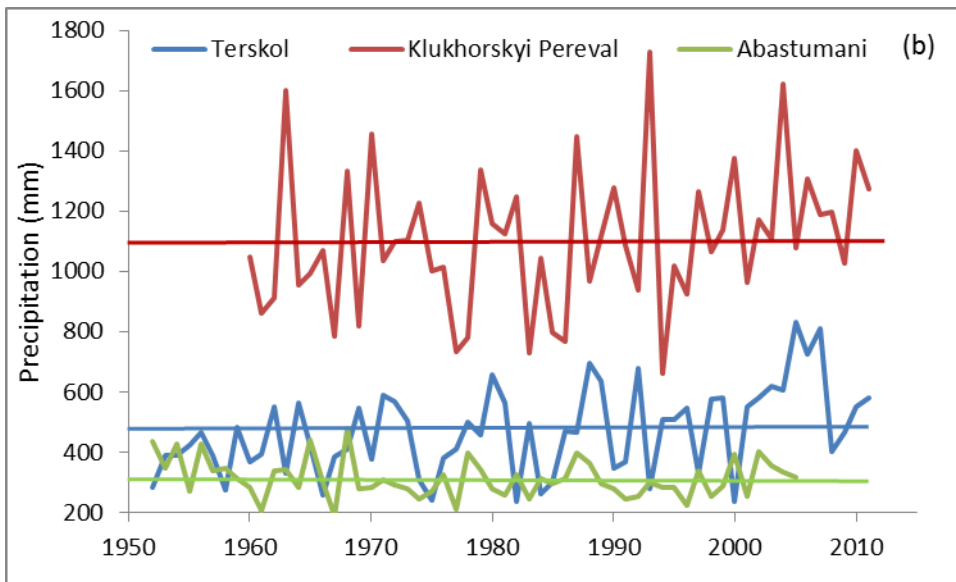
724 Figure 5. Expansion of exposed rocks on the southern slope of Mt. Elbrus: (a) 1999 and (b) 2012.

725 Arrows point at the expanded areas of exposed rocks. The 1999 Landsat ETM+ image (Table
726 1) is used as background.

727



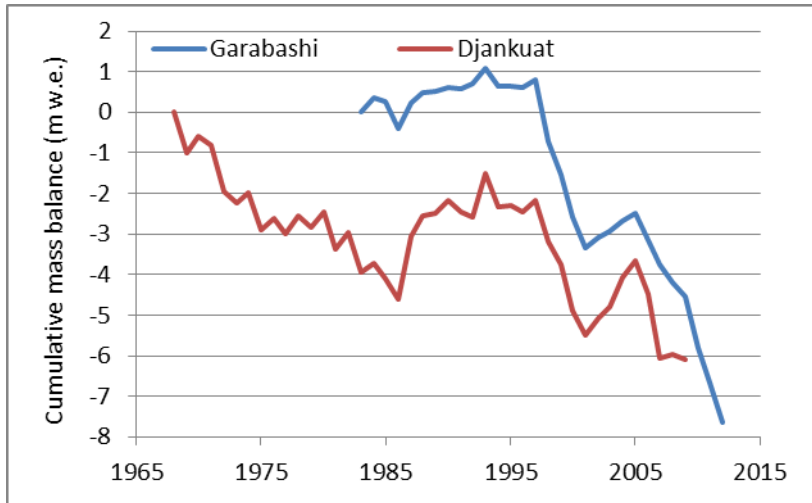
728



729

730 Figure 6. (a) JJA temperature and (b) October-April precipitation for Abastumani, Klukhorskyi
 731 Pereval and Terskol stations. Horizontal lines show record averages for each station.

732



733

734 Figure 7. Cumulative mass balance of Garabashi and Djankuat glaciers (WGMS, 2013;
735 unpublished records from the Institute of Geography, Russian Academy of Science for
736 Garabashi in 2012).

737

738

739